

# Excited-State Properties of the Four Stereoisomers of 1-(9-Anthryl)-4-phenyl-1,3-butadiene: Evidence of Adiabatic and Diabatic Deactivation Pathways

G. Bartocci, E. Marri, and A. Spalletti\*

Dipartimento di Chimica, Università di Perugia, 06123 Perugia, Italy

Received: June 12, 2002; In Final Form: August 2, 2002

The photophysics and photochemistry of the four geometrical isomers of 1-(9-anthryl)-4-phenyl-1,3-butadiene have been extensively studied by stationary and pulsed spectrometry in nonpolar solvent. Fluorimetric and laser flash techniques were used to measure the quantum yields and lifetimes of the lowest excited states of singlet and triplet multiplicity at different temperatures. This paper reports the spectral characterization of the four isomers and their derived parameters of the radiative, nonradiative, and reactive relaxation pathways. The isomerization proceeds through triplet diabatic and/or adiabatic mechanisms, generally with low quantum yield, owing to high torsional barriers in the  $S_1$  state and small  $T_1$  population quantum yields, due to the very fast  $S_1 \rightarrow S_0$  internal conversion. At high temperature, a singlet diabatic mechanism is also operative.

## Introduction

The excited-state properties of diarylethenes and diarylpolyenes have been the subject of wide investigation in the past decades. Particular attention has been given to the photophysics and photochemistry of short chain  $\alpha,\omega$ -diphenylpolyenes owing to their role as models for conformational properties and photoisomerization reactions about a polyene double bond in compounds of biological interest (proteins, visual pigments, etc.).<sup>1–4</sup> The ordering of the lowest excited states of  $A_g$  and  $B_u$  character, which is correlated with the length of the polyene chain, was particularly investigated, because it seems to be a relevant factor in the excited-state behavior of these molecules.

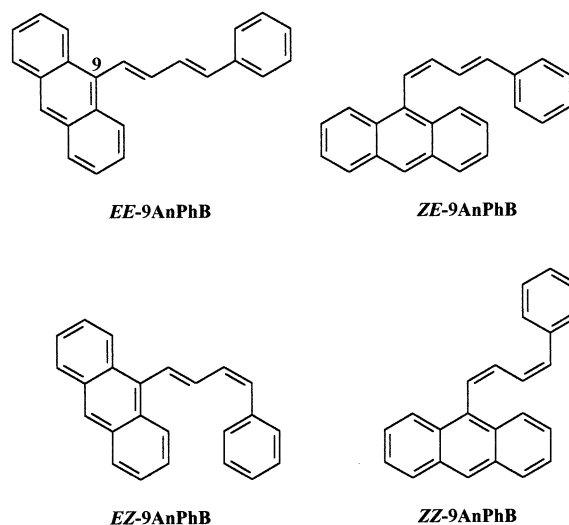
Diphenylbutadiene has been extensively investigated by theoretical and experimental approaches.<sup>1,3</sup> Much less is known about the corresponding asymmetric compounds where a phenyl ring is replaced by a larger polycyclic group. Previous results on the corresponding ethene derivatives<sup>2</sup> showed that the presence of larger polycyclic aromatic groups has strong effects on the relaxation pathways of the lowest excited states, leading to a decrease in the reactive process in  $S_1$  and an increase of the radiative and/or nonradiative deactivation. Moreover, these groups, such as naphthyl, phenanthryl, anthryl, etc., can open different photoreaction pathways to isomerization involving the triplet manifold and an adiabatic mechanism.<sup>5–8</sup>

Along the lines of our previous results, we recently turned to the study of some asymmetric diarylbutadienes  $Ar-CH=CH-CH=CH-phenyl$ , where  $Ar = 1$ -naphthyl,<sup>9</sup> 2-anthryl,<sup>10</sup> 9-phenanthryl,<sup>9</sup> 1-pyrenyl,<sup>9</sup> *n*-pyridyl,<sup>9,11</sup> and *n*-thienyl.<sup>9,12</sup>

In this paper we report the results for the excited-state properties of the four geometrical isomers of 1-(9-anthryl)-4-phenyl-1,3-butadiene (9AnPhB). Their spectral (absorption and emission) properties and the kinetics of the radiative and radiationless relaxation processes of the lowest excited states are discussed and compared with those of the corresponding ethene derivatives and of diphenyl-1,3-butadiene (DPhB) to have a general picture of the substituent and polyenic chain effects on the photobehavior of these asymmetric dienes.

\* To whom correspondence should be addressed. E-mail: faby@phch.chem.unipg.it.

## CHART 1



## Experimental Section

The compounds investigated (see Chart 1) prepared by standard methods by G. Galiazzo (Padua University), were purified by semipreparative HPLC. A Waters apparatus was used, equipped with a SymmetryPrep C18 (7  $\mu$ m) and an UV spectrophotometer as detector, using  $H_2O/CH_3CN$  mixtures as the eluant.

Most measurements were carried out in a mixture of methylocyclohexane and 3-methylpentane (MCH/3MP, 9:1 v/v), some others in cyclohexane (CH) and benzene. All solvents were from Fluka, spectrograde. MCH and 3MP were purified by standard procedures.

The absorption measurements were carried out with a Perkin-Elmer Lambda 16 spectrophotometer. The fluorescence spectra were measured by using a SPEX Fluorolog-2 F 112A1 spectrofluorimeter. The emission quantum yields were determined using 9,10-diphenylanthracene in CH as standard ( $\phi_F = 0.90$ ).<sup>13,14</sup> The values reported in the tables are averages of at least three independent experiments with a mean deviation of

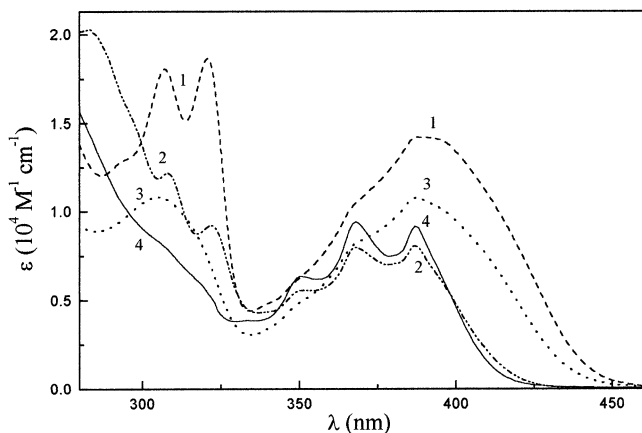


**Figure 1.** Absorption spectra of the four stereoisomers of 9AnPhB in MCH/3MP at room temperature: curves 1–4 refer to *EE*, *ZE*, *EZ*, and *ZZ*, respectively.

ca. 5%. The fluorescence lifetimes ( $\tau_F$ , mean deviation of three independent experiments, ca. 7%) were measured with both an Edinburgh Instruments 199S spectrofluorometer (single photon counting method) and a SPEX Fluorolog- $\tau 2$  system (phase modulation technique).

The triplet properties were investigated by laser flash photolysis at 355 nm (using the third harmonic of a Continuum Nd:YAG laser) and at 420 nm (using a parametric oscillator, OPO, pumped by the Nd:YAG laser) in biacetyl sensitized experiments.

For photochemical measurements, a 150 W high-pressure xenon lamp coupled with a monochromator was used. The reactions were monitored by HPLC. A ferrioxalate actinometer was used for the measurements of photoisomerization quantum yields. In the sensitized experiments, biacetyl in benzene was used as the triplet energy donor and the concentration of the acceptor was kept in the  $1.3 \times 10^{-4}$  to  $10^{-3}$  M range where both the conditions (100% of energy transfer from the triplet state of biacetyl and no occurrence of the quantum chain process involving energy transfer from  $^3E^*$  to  $^3Z^*$ ) are fulfilled. The solutions were deoxygenated by purging with nitrogen.

A cryostat (Oxford Instruments DN 1704) was used to control temperature in the 77–354 K range.

The 9AnPhB stereoisomers were characterized by their spectral and photochemical behavior, besides through the synthetic strategy and the analogy with the 2AnPhBs.<sup>10</sup> A comparison with the corresponding *E*- and *Z*-ethene derivatives was very useful (see below).

## Results and Discussion

**Spectral and Photophysical Properties.** *Absorption and Emission Spectra.* The absorption spectra of the four geometrical isomers of 9AnPhB in MCH/3MP at room temperature are shown in Figure 1. They are characterized by two main bands. The first one in the 340–440 nm region has a well resolved vibronic structure for the *ZE* and *ZZ* isomers with a progression of ca.  $1450 \text{ cm}^{-1}$ , as previously observed for *Z*-9-styrylanthracene (*Z*-9StAn),<sup>15</sup> which points to an anthracenic nature of the excited singlet state involved.

In the case of the isomers with the anthryl group in trans position (*EE* and *EZ* isomers), the first band of the absorption spectrum is broad, as previously found for *E*-9StAn.<sup>15,16</sup> For these isomers, the absence of a well defined vibronic structure could be due to the presence of a set of different geometries concurring to absorption. The second one, probably of the

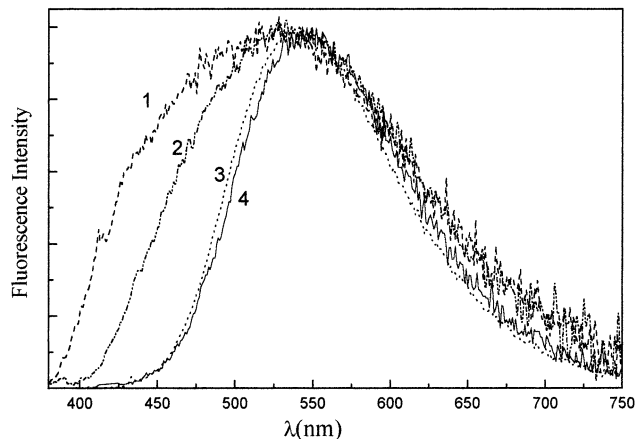


**Figure 2.** Normalized fluorescence spectra of the four stereoisomers of 9AnPhB in MCH/3MP at room temperature: curves 1–4 refer to *ZZ*, *ZE*, *EE*, and *EZ*, respectively.

styrene type, is localized in the 250–330 nm region. These spectral results, together with the blue shift (about 20 nm) and lower absorption intensity observed for the two isomers with the anthryl group in the *cis* position, indicate a more localized electronic excitation on the polycyclic chromophore probably because of a more distorted geometry of the *ZE* and *ZZ* isomers, if compared to *EE* and *EZ*, related to steric interactions in the ground and excited states.

The fluorescence spectra of the four isomers in MCH/3MP at room temperature are shown in Figure 2. They are bell-shaped and those of the *ZE* and *ZZ* isomers are more extended with the maximum substantially blue-shifted (about 20 nm) with respect to those of *EZ* and *EE*, as observed in the absorption spectra. The Stokes shifts are large (about 150 nm) for all the isomers, as found for 9StAn. This spectral behavior could be due to solute–solvent interactions in the lowest singlet excited state, which results in a relaxed non-Franck Condon state.

An important temperature effect was found on the spectra, particularly on the absorption properties. In fact, the absorption spectra of all the isomers change in shape and intensity with decreasing temperature, particularly for *EE* and *ZZ* (see Figure 3). The decrease of temperature leads to an absorption spectrum shifted toward the red and to a change in the intensity distribution of the vibronic components. This behavior, already observed for the trans isomers of stilbene,<sup>17</sup> diarylbutadienes,<sup>9,10</sup> and aza derivatives of diarylethenes,<sup>18</sup> has been explained on the basis of excitation of sets of different ground-state species more or less deviating from planarity. Decreasing temperature and increasing viscosity favor the planar or quasi-planar forms leading to red-shifted and more resolved spectra and to a larger vibronic progression. Meanwhile, the emission spectrum does not change too much in shape and position on decreasing temperature. Only at 77 K, in the rigid matrix does the spectra markedly shift toward the blue (50–60 nm), as shown in Figure 4, so reducing by 80–100 nm the Stokes shifts if compared with those observed at room temperature. This behavior, in agreement with a relaxed (non-Franck–Condon)  $S_1$  state, confirms the hypothesis that solvation is responsible for the marked Stokes shifts, observed at room temperature.

The fluorescence excitation spectrum, which reproduces the absorption spectrum, and that of emission are independent of the emission and excitation wavelengths, respectively, at any temperature for all the isomers. These results, together with a monoexponential fluorescence decay and with the fluorescence quantum yield independent of  $\lambda_{exc}$  (see later), seem to rule out

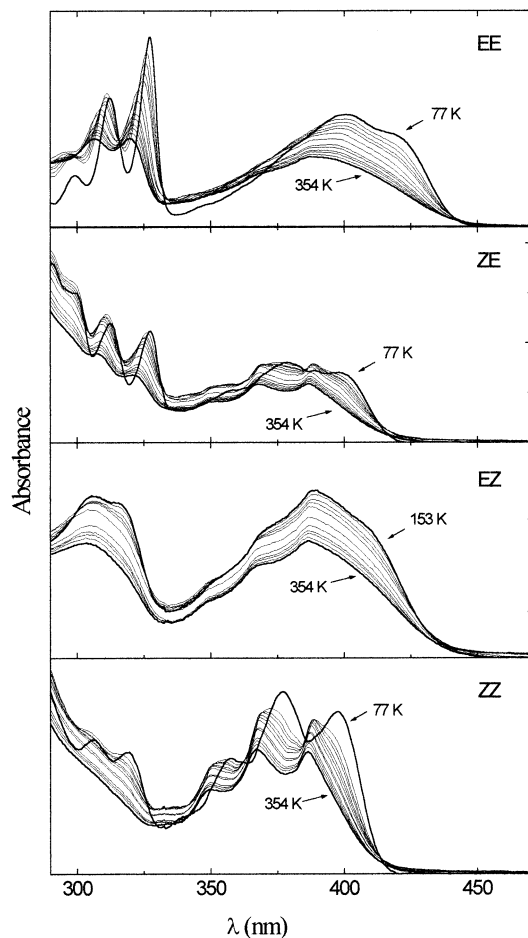


**Figure 3.** Absorption spectra of the four stereoisomers of 9AnPhB in MCH/3MP as a function of temperature.

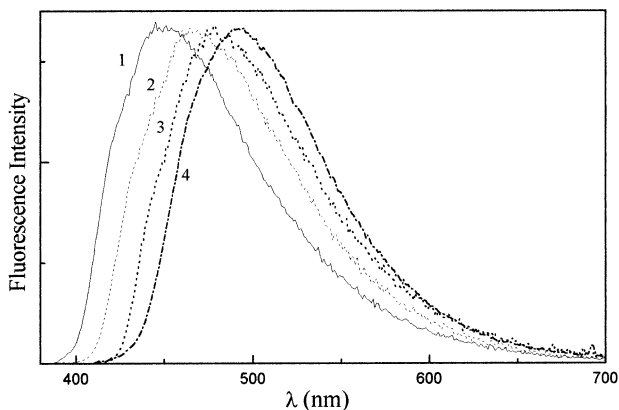


**Figure 4.** Normalized fluorescence spectra of the four stereoisomers (curves 1–4 refer to ZZ, ZE, EZ, and EE, respectively) of 9AnPhB in MCH/3MP at 77 K.

the involvement of detectable conformational equilibria in the photobehavior of these molecules.

**Fluorescence Properties.** Table 1 shows the fluorescence quantum yields and lifetimes of the four geometrical isomers of 9AnPhB in MCH/3MP at room temperature and the kinetic parameters for the competitive relaxation pathways. The non-radiative rate parameter ( $k_{NR}$ ) includes the singlet contribution to isomerization in  $S_1$ , the  $S_1 \rightarrow T_1$  intersystem crossing (ISC), and the  $S_1 \rightarrow S_0$  internal conversion (IC) processes.

The radiative rate parameter ( $k_F = \phi_F/\tau_F$ ) ( $(2-3) \times 10^7 \text{ s}^{-1}$ ) of all the isomers decreases by almost 1 order of magnitude relative to that of the analogous ethene ( $1 \times 10^8 \text{ s}^{-1}$ ), thus

**TABLE 1: Fluorescence Quantum Yield ( $\phi_F$ ), Lifetime [ $\tau_F$  (ns)], and Radiative [ $k_F$  and  $k_F^0$  ( $10^7 \text{ s}^{-1}$ )] and Nonradiative [ $k_{NR}$  ( $10^7 \text{ s}^{-1}$ )] Rate Constants of the 9AnPhB Stereoisomers, in MCH/3MP at Room Temperature<sup>a</sup>**

isomer	$\phi_F$	$\tau_F$ (ns)	$k_F$	$k_{NR}$	$k_F^0$
EE	0.22	6.9	3.2	11.3	22
EZ	0.15	5.6	2.7	15.2	16
ZE	0.073	4.5	1.6	20.6	13
ZZ	0.072	3.2	2.2	29.0	14
<i>E</i> -9StAn <sup>b</sup>	0.44	3.6	12.0	15.8	16
<i>Z</i> -9StAn <sup>c</sup>	0.19	2.2	9.0	36.5	12

<sup>a</sup> The parameters of the corresponding ethene derivatives are reported for comparison. <sup>b</sup> From ref 2. <sup>c</sup> From ref 8.

**TABLE 2: Spectral and Photophysical Properties of the Triplet State of *EE*-9AnPhB and *E*-9StAn (for Comparison), in Nonpolar Solvents at Room Temperature**

compound	solvent	$\lambda_{max}$ (nm)	$\tau_T$ ( $\mu\text{s}$ )	$\epsilon_{T,max}$ ( $\text{M}^{-1} \text{ cm}^{-1}$ )	$\phi_T$
<i>EE</i> -9AnPhB	MCH/3MP	350, 480	25	10 600, 12 940	0.39
	benzene	480	30	13 090	0.39
<i>E</i> -9StAn <sup>a</sup>	benzene	460	45	21 000	0.32

<sup>a</sup> From ref 15.

indicating an inversion in the ordering of the two lowest excited singlet states in the diene compound. In the latter, the  $S_1$  state assumes an  $L_b$  nature and the  $S_1 \rightarrow S_0$  radiative transition becomes partially allowed by vibronic coupling with the closely located  $S_2$  state of ( $L_a-B_u$ ) nature. For comparison, in Table 1 the radiative rate constant ( $k_F^0$ ) is also reported, as obtained by the approximate natural lifetime ( $\tau_F^0$ ), calculated from the integral of the absorption intensity using the modified Strickler–Berg relationship:<sup>19</sup>

$$k_F^0 = 1/\tau_F^0 = 2.88 \times 10^{-9} (\bar{\nu}_{00} n_s)^2 \int \epsilon(\bar{\nu}) d\bar{\nu} \quad (1)$$

where  $n_s$  is the refractive index of the solvent and  $\bar{\nu}_{00}$  is the 00 vibronic component of the allowed transition, which is considered the main factor responsible for absorption. The  $k_F^0$  value increases with increasing the length of the polyene chain, as previously observed in the diphenyl-<sup>1a</sup> and dithienylpolyenes.<sup>12</sup>

Table 1 shows how the presence of the anthryl group can affect the excited-state properties and in particular the  $k_F$  value of the 9AnPhB isomers. The latter markedly decreases and differs from the  $k_F^0$  value, when compared with the phenyl analogues. This further confirms the different nature of the excited states implied in the absorption ( $^1L_a-B_u$ )\* and emission ( $^1L_b$ )\* processes in 9AnPhBs.

The rate parameter of the nonradiative processes ( $k_{NR}$ ), derived from the fluorescence lifetime and quantum yield [ $k_{NR} = (1 - \phi_F)/\tau_F$ ], points out that such deactivation pathways are much more relevant than the radiative one, as previously observed for the ethene analogues, particularly for the Z isomer.

**Triplet Properties.** Table 2 collects the information on the triplet state of the *EE* isomer obtained by laser flash photolysis at room temperature in de-oxygenated MCH/3MP and benzene solutions. The  $T_1-T_n$  spectrum in MCH/3MP is shown in Figure 5.

The triplet quantum yield,  $\phi_T$ , was found to be substantial (0.39) in both solvents and higher than the value obtained for *E*-9StAn.<sup>15,20</sup>

The long triplet lifetime ( $\tau_T$ , about 30  $\mu\text{s}$ ), peculiar of nontwisting states, points to high torsional barriers in  $T_1$  and to a prevalent nonreactive and nonradiative relaxation, as found for the ethene analogue.<sup>2</sup>

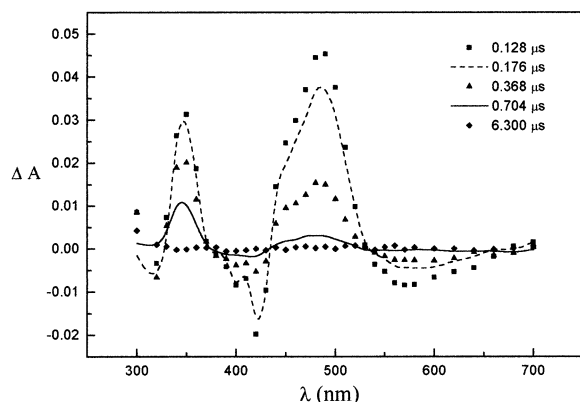


**Figure 5.**  $T_1-T_n$  absorption spectra of  $EE$ -9AnPhB in MCH/3MP at room temperature, obtained at different delay times.

**TABLE 3: Direct and Biacetyl Sensitized Photoisomerization Quantum Yields of the 9AnPhB Stereoisomers in MCH/3MP and Benzene, Respectively, at Room Temperature**

isomer	direct			sensitized		
	$\phi_{EE}$	$\phi_{EZ}$	$\phi_{ZE}$	$\phi_{EE}$	$\phi_{EZ}$	$\phi_{ZE}$
$ZE$	0.039			0.75		
$EZ$	0.071			0.83		
$ZZ$	0.035	0.010	0.024	0.58	0.12	

The  $T_1-T_n$  absorption spectrum of the other isomers is not observed at room temperature in deaerated fluid solutions. For direct excitation of these cis isomers, one obtains the same  $T_1-T_n$  absorption spectrum and triplet lifetimes (within the experimental error) of the  ${}^3EE^*$  transient, so suggesting the possible involvement of a triplet adiabatic pathway in the deactivation processes of cis isomers.

**Photochemical Behavior.** Table 3 collects the experimental quantum yields for the direct and photosensitized isomerization of the 9AnPhB isomers in MCH/3MP and benzene, respectively, at room temperature. The results indicate that (i) the  $EE$  isomer is not reactive even after long irradiation times, the electron distribution in the diene chain being such as to induce high torsional barriers at both the double bonds, (ii)  $EZ$  and  $ZE$  produce only  $EE$  with a low quantum yield (about 4–7%), and (iii) by direct irradiation, the  $ZZ$  isomer gives rise to all the other isomers with a quantum yield of about 1–3%, whereas only  $EE$  and  $EZ$  are generated by triplet sensitization.

The formation (proportional to the irradiation time) of the  $EE$  photoproduct by direct and sensitized excitation of  $ZZ$ -9AnPhB suggests the involvement of at least one triplet adiabatic process through a “one photon-two bonds” isomerization mechanism.<sup>11,21</sup>

The high photoisomerization quantum yield, sensitized by biacetyl (about 0.8 in deaerated benzene solutions at room temperature for  $EZ$ ,  $ZE$ , and  $ZZ$ ), indicates a large reactivity of their triplet state. On the contrary, the triplet state of  $EE$  is not reactive, as previously observed in the case of  $E$ -9StAn,<sup>2</sup> owing to a high torsional barrier also in the triplet state and/or to the presence of an adiabatic process in the reverse direction.

The limiting quantum yield for the photosensitized isomerization ( $\phi_{ISO,X}^{sens}$ , where  $X = ZE, EZ,$  and  $ZZ$ ), are larger than 0.5 (value generally found for the diabatic triplet mechanism)<sup>2</sup> and lower than 1.0 (characteristic value of the adiabatic triplet mechanism in dilute solutions).<sup>8,10,22,23</sup> These values can be explained by the involvement of both diabatic and adiabatic processes in the deactivation of the perpendicular triplet excited state and/or by the competition of  $T_1 \rightarrow S_0$  intersystem crossing

with the torsional pathway in the deactivation of the planar  $T_1$  state. Because the torsional process is expected to be very fast because the triplet lifetime is not quenched by oxygen (see below), diabatic and adiabatic reactive pathways must be involved in the  $T_1$  deactivation mechanisms of the mixed ( $EZ$  and  $ZE$ ) and  $ZZ$  isomers.

Then  $\phi_{ISO,X}^{sens}$  can be expressed as

$$\phi_{ISO,X}^{sens} = {}^3\phi_{ISO,X}^{sens,ad} + {}^3\phi_{ISO,X}^{sens,d} \quad (2)$$

where  ${}^3\phi_{ISO,X}^{sens,ad}$  and  ${}^3\phi_{ISO,X}^{sens,d}$  indicate the adiabatic and diabatic contributions, respectively, to the experimental quantum yield for the photosensitized isomerization.

The quantum yield for the diabatic photosensitized isomerization leading to  $EE$  [ ${}^3perpE^* \rightarrow {}^1perpE \rightarrow \alpha{}^1EE + (1-\alpha){}^1ZE$  or  ${}^3Eperp^* \rightarrow {}^1Eperp \rightarrow \alpha{}^1EE + (1-\alpha){}^1EZ$ ]:

$${}^3\phi_{ISO,X}^{sens,d} = (1 - {}^3\phi_{ISO,X}^{sens,ad})\alpha \quad (3)$$

where  $\alpha$  represents the fraction of molecules which decay to  $EE$  in the ground state from the perpendicular configuration. Assuming that  $\alpha$  is 0.5, as for diphenylpolyenes (DHPs)<sup>24</sup> and dithienylpolyenes (DTPs),<sup>12</sup> values of 0.50 and 0.66 were derived for the adiabatic contribution of the photoreactive mechanism in  $T_1$  for the  $ZE$  and  $EZ$  isomers, respectively, by the equation:

$${}^3\phi_{ISO,X}^{sens,ad} = ({}^3\phi_{ISO,X}^{sens} - \alpha)/(1 - \alpha) \quad (4)$$

After direct irradiation of dilute de-oxygenated solutions of  $ZZ$ -9AnPhB in MCH/3MP at room temperature, the HPLC analysis showed the formation of the other three isomers,  $EE$  being the main photoproduct. The appearance of  $EE$  during the first irradiation times in both the direct and sensitized experiments, indicates the involvement of “one photon-two bonds” isomerization that implies the presence of almost one adiabatic process. In the direct photoreaction, the  $ZZ \rightarrow EE$  process takes place through a triplet mechanism, involving an adiabatic  ${}^3ZZ^* \rightarrow {}^3EZ^*$  and a mixed diabatic [ ${}^3EZ^* \rightarrow {}^3Eperp^* \rightarrow {}^1Eperp \rightarrow \alpha{}^1EE + (1-\alpha){}^1EZ$ ] and adiabatic ( ${}^3EZ^* \rightarrow {}^3Eperp^* \rightarrow {}^3EE^* \rightarrow {}^1EE$ ) pathways. This was suggested by the photoreactive behavior of  ${}^3EZ^*$  and by the lack of the emissive component of  $EZ$  in the measured emission spectra of  $ZZ$ .

The quantum yield for the adiabatic  ${}^3ZZ^* \rightarrow {}^3EZ^*$  process can be evaluated by

$${}^3\phi_{ZZ-EZ}^{ad} = \phi_{ZZ-EE}^{sens} / \phi_{EZ-EE}^{sens} \quad (5)$$

On the contrary, the  $ZZ \rightarrow ZE$  direct photoisomerization proceeds through a singlet mechanism, because  $ZE$  was not formed by triplet sensitization,  $\phi_{ZZ-ZE}$  increased with increasing temperature (see below) and the emissive component of  $ZE$  was not observed by exciting the  $ZZ$  isomer.

The  $S_1 \rightarrow T_1$  intersystem crossing quantum yield of the mixed ( $EZ$  and  $ZE$ ) and  $ZZ$  isomers was derived by

$$\phi_{ISC,X} = \phi_{X-EE} / \phi_{X-EE}^{sens} \quad (X = EZ, ZE, \text{ and } ZZ) \quad (6)$$

Values of 0.085, 0.056, and 0.060 were derived for  $\phi_{ISC}$  of the  $EZ$ ,  $ZE$ , and  $ZZ$  isomers, respectively, in nonpolar solvent at room temperature.

**Oxygen Effect.** Table 4 shows the oxygen effect on the fluorescence parameters ( $\phi_F$  and  $\tau_F$ ) and on the direct cis  $\rightarrow$  trans photoprocess of the 9AnPhB isomers.

The photoreactivity of these molecules is markedly dependent on oxygen. In fact, in oxygen-saturated solutions the quantum



**TABLE 4: Oxygen Effect on Fluorescence Lifetime (ns) and Photoisomerization Quantum Yield of the 9AnPhB Stereoisomers in MCH/3MP at Room Temperature**

isomer	[O <sub>2</sub> ] = 0 M					[O <sub>2</sub> ] = 2.6 × 10 <sup>-3</sup> M <sup>a</sup>					[O <sub>2</sub> ] = 12.3 × 10 <sup>-3</sup> M <sup>a</sup>				
	φ <sub>F</sub>	τ <sub>F</sub>	φ <sub>EE</sub>	φ <sub>EZ</sub>	φ <sub>ZE</sub>	φ <sub>F</sub>	τ <sub>F</sub>	φ <sub>EE</sub>	φ <sub>EZ</sub>	φ <sub>ZE</sub>	φ <sub>F</sub>	τ <sub>F</sub>	φ <sub>EE</sub>	φ <sub>EZ</sub>	φ <sub>ZE</sub>
EE	0.22	6.9				0.16	5.4				0.09	2.8			
ZE	0.073	4.5	0.039			0.06	3.9	0.14			0.04	2.3	0.32		
EZ	0.15	5.6	0.071			0.11	4.4	0.047			0.07	2.5	0.028		
ZZ	0.072	3.2	0.035	0.010	0.024	0.058	2.4	0.026	0.067	0.013	0.046	1.7	0.025	0.30	0.006

<sup>a</sup> From ref 25.**TABLE 5: Temperature Effect on Fluorescence Quantum Yields, Lifetime (ns) and Kinetic Parameters (10<sup>7</sup> s<sup>-1</sup>) of the Four Isomers of 9AnPhB in MCH/3MP**

T (K)	EE				EZ				ZE				ZZ								
	φ <sub>F</sub>	τ <sub>F</sub>	k <sub>F</sub>	k <sub>IC</sub>	φ <sub>F</sub>	φ <sub>EE</sub>	τ <sub>F</sub>	k <sub>F</sub>	k <sub>IC</sub>	φ <sub>F</sub>	φ <sub>EE</sub>	τ <sub>F</sub>	k <sub>F</sub>	k <sub>IC</sub>	φ <sub>F</sub>	φ <sub>EZ</sub>	φ <sub>EE</sub>	τ <sub>F</sub>	k <sub>F</sub>	k <sub>IC</sub>	
354	0.20	7.0	2.8	5.9	0.12	0.10	5.1	2.3	14	0.064	0.072	4.2	1.5	20.7	0.055	0.10	0.014	0.044	3.1	1.8	22.6
313					0.14		5.5	2.5	13.5	0.071	0.049	4.4	1.6	20.7	0.067				3.2	2.0	25.8
293	0.22	6.9	3.2	5.7	0.15	0.071	5.6	2.7	13	0.073	0.039	4.5	1.6	19.3	0.072	0.012	0.024	0.035	3.2	2.2	26.6
253	0.26	7.3	3.6	4.5	0.16		6.1	2.7	12	0.077		4.8	1.6	17.9	0.077				3.9	2.0	22.0
213					0.18		6.4	2.9	11	0.082		4.9	1.6	17.5	0.089				4.0	2.2	21.0
153	0.32	7.4	4.3	3.6						0.11				14.4	0.12				4.6	2.7	17.3
77	0.64	6.9	9.3							0.63		7.4	8.5	3.7	0.58				5.8	10	5.5

yield of the  $ZE \rightarrow EE$  and  $ZZ \rightarrow EZ$  processes increases up to 1 order of magnitude, whereas it decreases for the other cis  $\rightarrow$  trans processes.

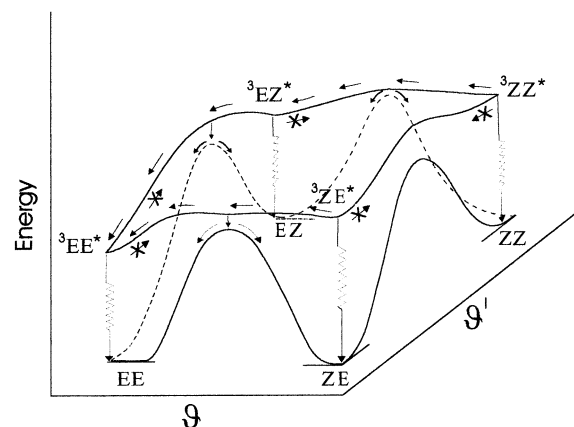
The fluorescence quantum yield and the lifetime decrease with increasing oxygen concentration, whereas the  $k_F$  value of all the isomers is independent of oxygen.

The different behavior of  $\phi_F$  and  $\phi_{ISO}$  with respect to the oxygen effect (see Table 4) suggests that different excited states are involved in the radiative and reactive processes and that the lowest triplet state of these isomers should have a very different lifetime.

A reliable interpretation of these results can be proposed by considering that oxygen can affect the  $S_1 \rightarrow T_1$  (ISC) and  $T_1 \rightarrow S_0$  (ISC') intersystem crossing processes to different extents, as expected from the nonradiative transition theory. For all the isomers the oxygen effect produces a larger increase of the  $k_{ISC,X}$  than the  $k_{ISC',X}$  rate constant owing to a lower energy gap between  $S_1$  and  $T_1$  with respect to that between  $T_1$  and  $S_0$ , thus increasing the population of the reactive excited species in the  $T_1$  state, in agreement with the decrease of the fluorescence lifetime.

Furthermore, the lifetime of  ${}^3ZE^*$  and  ${}^3ZZ^*$  must be very short because these species were not observed after the laser pulse even in oxygen-free solutions, thus suggesting a relatively low torsional barriers. These species are expected to be located at a very shallow minimum and to undergo twisting more rapidly than they are quenched by oxygen. In the case of the  $EZ$  isomer, the decrease of the  $EZ \rightarrow EE$  quantum yield, in oxygen-saturated solutions, indicates that  ${}^3EZ^*$  is quenched by oxygen owing to a longer lifetime. Accordingly,  $\phi_{ZZ \rightarrow EZ}$  markedly increases to the detriment of  $\phi_{ZZ \rightarrow EE}$ , in oxygen-saturated solutions, also in agreement with our hypothesis that the  $EE$  isomer is photoproduced from  $ZZ$  by the adiabatic  ${}^3ZZ^* \rightarrow {}^3EZ^*$  process.

On the basis of the (i) the different oxygen effect on  $\phi_{ISO}$  and  $\phi_F$ , (ii) the practically temperature-independence of  $\tau_F$  (see below), and (iii) the absence of the emissive components of the excited species  ${}^1EE^*$  and/or  ${}^1EZ^*$  and/or  ${}^1ZE^*$ , adiabatically produced, in the fluorescence spectrum of the isomers of 9AnPhB, one can conclude that the involvement of the singlet pathways in the cis  $\rightarrow$  trans photoreaction should be excluded (except for  $ZZ \rightarrow ZE$ ) and that the photoisomerization proceeds mainly through a triplet mechanism in MCH/3MP at room temperature, as proposed in the sketch of Figure 6.

**Figure 6.** Qualitative sketch of the potential energy curves as a function of the rotation around the two double bonds for the four isomers of 9AnPhB in the triplet manifold.

**Temperature Effect.** Table 5 shows the effect of temperature on the photophysical and photochemical parameters and on the rate constants of the radiative and nonradiative deactivation processes of the  $S_1$  state of the 9AnPhB isomers. The fluorescence lifetime of the isomers with the anthryl group in the trans position is practically independent of temperature, whereas those with the anthryl group in the cis position show an increase of  $\tau_F$  with decreasing temperature, particularly high in a rigid matrix at 77 K. The fluorescence quantum yield of all the isomers increases markedly with decreasing temperature, particularly for the  $ZE$  and  $ZZ$  isomers. The photoreactivity of  $EE$  was not observed, even at high temperature, whereas that of all the other isomers increases at  $T > 300$  K, even if it remains always very low (4–10%).

These results suggest the contribution of a singlet mechanism, with a high torsional barrier, in the  $ZE \rightarrow EE$ ,  $EZ \rightarrow EE$ , and  $ZZ \rightarrow ZE$  photoisomerization in nonpolar solvent at high temperature. Furthermore, they confirm that the  $ZZ \rightarrow EZ$  process proceeds only through a triplet mechanism also at 354 K.

The Arrhenius-type plots, based on the fluorescence yields and lifetimes, could lead to incorrect values of the frequency factor and torsional barrier of the activated reactive pathway in  $S_1$ , because these derived parameters could be a combination of those for both the activated processes (isomerization and

**TABLE 6: Photophysical Properties of *EE*-9AnPhB in Different Solvents at 293 K (Dielectric Constant, *D*, Polarizability,  $\alpha_s$ , and Viscosity,  $\eta$ , of the Solvents)**

solvent	<i>D</i>	$\alpha_s$	$10^3\eta$ (Pa s)	$\phi_F$	$\tau_F$ (ns)	$10^{-7}k_F$ (s <sup>-1</sup> )
carbon disulfide	2.64	0.354	0.363	0.41	4.2	9.8
toluene	2.38	0.292	0.5859	0.38	6.2	6.1
MCH/3MP	2.01	0.252	0.691	0.22	6.9	3.2
isopentane	1.83	0.217	0.225	0.19	7.1	2.7
perfluorohexane: <i>n</i> -hexane (3:1)		0.183		0.13	7.0	1.9

internal conversion). More reliable values of the Arrhenius parameters for the activated rotation can be obtained by

$$\ln {}^1k_{X^* \rightarrow \text{perp}^*}(T) = \ln {}^1A_{X^* \rightarrow \text{perp}^*} - {}^1\Delta E_{X^* \rightarrow \text{perp}^*}/RT \quad (7)$$

where  ${}^1k_{X^* \rightarrow \text{perp}^*}$  is the kinetic constant of the  ${}^1X^* \rightarrow {}^1\text{perp}^*$  torsional process ( $X = ZE, EZ,$  and  $ZZ$ ). The  ${}^1k_{X^* \rightarrow \text{perp}^*}(T)$  values at the explored temperatures were derived for the  ${}^1ZZ^* \rightarrow {}^1Z\text{perp}^*$  process by

$${}^1k_{X^* \rightarrow \text{perp}^*}(T) = {}^1k_{ZZ^* \rightarrow Z\text{perp}^*}(T) = \phi_{ZZ \rightarrow ZE}(T)/\alpha\tau_{F,ZZ}(T) \quad (8)$$

being  $\phi_{ZZ \rightarrow ZE}(T) = {}^1\phi_{ZZ \rightarrow ZE}(T)$ , whereas for the  ${}^1EZ^*$  (or  ${}^1ZE^*$ )  $\rightarrow {}^1E\text{perp}^*$  (or  ${}^1\text{perp}E^*$ ) and  ${}^1ZZ^* \rightarrow {}^1\text{perp}Z^*$  processes,

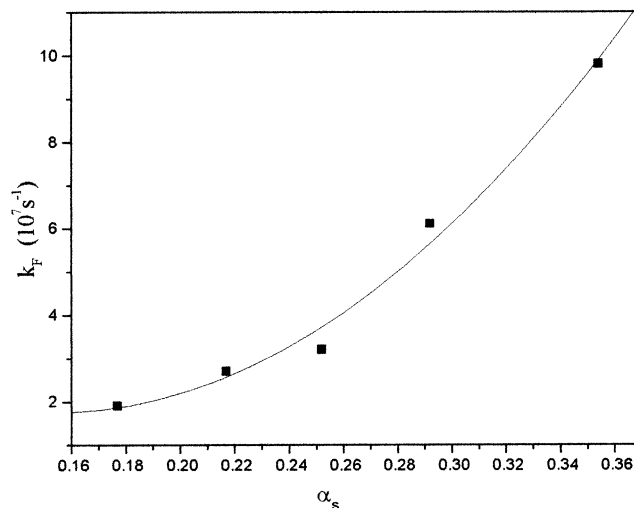
$${}^1k_{X^* \rightarrow \text{perp}^*}(T) = [\phi_{\text{ISO},X}(T) - k_{\text{ISC},X}\tau_{F,X}(T)\phi_{\text{ISO},X}^{\text{sens}}]/\alpha\tau_{F,X}(T) \quad (9)$$

was used, where  $k_{\text{ISC},X} = \phi_{\text{ISC},X}/\tau_{F,X}$  was assumed temperature independent.

The Arrhenius parameters  ${}^1A_{X^* \rightarrow \text{perp}^*} = 2 \times 10^{12}$  and  $1.1 \times 10^{12} \text{ s}^{-1}$  and  ${}^1\Delta E_{X^* \rightarrow \text{perp}^*} = 7.3$  and  $7.9 \text{ kcal/mol}$  were derived from the plot of eq 7 for the  ${}^1ZZ^* \rightarrow {}^1Z\text{perp}^*$  and  ${}^1ZE^* \rightarrow {}^1\text{perp}E^*$  processes, respectively. Torsional barrier values of 8.4 and 9.0 kcal/mol were roughly estimated for the *EZ* isomer and for the  ${}^1ZZ^* \rightarrow {}^1\text{perp}Z^*$  process, respectively, assuming a mean value of the frequency factor of  $1.6 \times 10^{12} \text{ s}^{-1}$ .

The radiative rate parameter is practically independent of temperature for the mixed (*EZ* and *ZE*) and *ZZ* isomers. The small changes in  $k_F$  with temperature for these molecules are due to the well-known dependence of the radiative rate constant on the refractive index of solvent,  $n_s$ .<sup>26</sup> In the case of *EE*-9AnPhB, a relevant increase of  $k_F$  with decreasing temperature was observed in fluid solutions. This behavior can be due to the dependence of the radiative rate parameter on the solvent polarizability,  $\alpha_s = (n_s^2 - 1)/(n_s^2 + 2)$ , as previously observed for *all-trans*-diphenylbutadienes<sup>1a,27,28</sup> and -dithienylbutadienes.<sup>12</sup>

Table 6 shows the polarizability effect on the fluorescence properties of *EE*-9AnPhB at room temperature. The  $\phi_F$  values increase, and those of  $\tau_F$  decrease with increasing the  $\alpha_s$  value. These findings indicate that the  $k_F$  values increase in a more polarizable solvent, thus supporting that (i) fluorescence of this isomer originates from a  ${}^1L_b^*$  state that contains (at room temperature and in low-polarizability solvents, such as perfluorohexane-*n*-hexane mixtures) a high degree of ( $L_a$ - $B_u$ ) character and (ii) the increase of  $\alpha_s$  leads to a smaller  $S_1$ - $S_2$  energy gap, thus increasing the mixing of an allowed  $S_2$  state, as  ${}^1(L_a$ - $B_u)^*$ , into a lowest forbidden state, as  ${}^1L_b^*$ , which increases  $k_F$ .<sup>27</sup> These findings confirm the results obtained for *EE*-di(2-thienyl)-butadiene<sup>12</sup> and those of previous calculations,<sup>29</sup> which indicate that only the mixing between a lowest forbidden and a higher allowed excited state has a noticeable effect on the natural lifetime,  $\tau_F^0$ .

**Figure 7.** Plot of  $k_F$  as a function of  $\alpha_s$  for *EE*-9AnPhB.**TABLE 7: Rate Constants ( $10^7 \text{ s}^{-1}$ ) of the Deactivation Processes of the Lowest Excited Singlet State of the 9AnPhB Stereoisomers in MCH/3MP at 293 K<sup>a</sup>**

compound	$k_F$	$k_{\text{ISC}}$	${}^1k_p^*$	$k_{\text{IC}}$
<i>EE</i>	3.2	5.6		5.7
<i>EZ</i>	2.7	1.8	0.087	13.0
<i>ZE</i>	1.6	1.2	0.14	19.3
<i>ZZ</i>	2.2	1.7	0.031 <sup>b</sup>	26.6
			0.72 <sup>c</sup>	
<i>E</i> -9StAn <sup>d</sup>	12.0	8.9	-	6.9
<i>Z</i> -9StAn <sup>e</sup>	9.0	7.8	6.0	22.7
<i>EE</i> -DPhB <sup>f</sup>	74.0	3.5	38.6	63.0

<sup>a</sup> The parameters of the corresponding ethene derivatives and those of DPhB are reported for comparison. <sup>b</sup> Related to  ${}^1ZZ^* \rightarrow {}^1\text{perp}Z^*$  process. <sup>c</sup> Related to  ${}^1ZZ^* \rightarrow {}^1Z\text{perp}^*$ . <sup>d</sup> From ref 2. <sup>e</sup> From ref 8. <sup>f</sup> From ref 1a.

The  $k_F$  values in Table 6 show a nonlinear trend with  $\alpha_s$  (see Figure 7), in agreement with the dependence of  $k_F$  on the  $S_1$ - $S_2$  energy gap [ $k_F \propto \Delta E(S_1-S_2)^{-2}$ ], as found for the *all-trans*-isomer of diphenylhexatriene<sup>27,28</sup> and di(2-thienyl)butadiene.<sup>12</sup> In the other isomers of 9AnPhB,  $k_F$  was found not to depend on the solvent polarizability, probably because of a larger  $S_1$ - $S_2$  energy gap, which reduces the mixing between the two states. This hypothesis is also confirmed by the lower  $k_F$  values found for these isomers with respect to *EE*.

In the rigid matrix at 77 K, a large increase of  $k_F$  was observed for all the isomers, which is mainly due to more-planar geometries in the  $S_1$  state, generated by the high viscosity of the matrix.

The nonradiative rate parameter markedly decreases with decreasing temperature, particularly for the isomers with the anthryl group in the *cis* position. On the basis of the Arrhenius parameters, the rate parameters for the activated reactive process in  $S_1$  were obtained at the explored temperatures. The  $k_{\text{IC},X}$  values as a function of temperature were derived by

$$k_{\text{IC},X}(T) = [1/\tau_{F,X}(T) - (k_{F,X} + k_{\text{ISC},X} + {}^1k_{X^* \rightarrow \text{perp}^*}(T))] \quad (10)$$

The results show a relevant temperature effect on the IC process (see below).

**Kinetic Parameters.** Table 7 collects the rate constants of the radiative and nonradiative [rotation ( ${}^1k_p^*$ ), intersystem crossing ( $k_{\text{ISC}}$ ), and internal conversion ( $k_{\text{IC}}$ )] processes of the  $S_1$  deactivation of all the 9AnPhB geometrical isomers and of those of 9StAn and DPhB for comparison, in nonpolar fluid solutions at 293 K.

As found for 9StAn<sup>2,8</sup> and DPhB,<sup>1a</sup> the main deactivation pathways of the S<sub>1</sub> state of 9AnPhBs are the nonradiative processes. Furthermore, in contrast with DPhB, whose S<sub>1</sub> state shows a fast reactive deactivation channel, the 9AnPhB stereoisomers and the ethene analogues show fast radiationless decay through IC. This deactivation channel, particularly important for ZE and ZZ, could be due to the two effective vibrational modes acting as coupling modes between S<sub>1</sub> and S<sub>0</sub>, namely the Franck–Condon active C=C stretching vibration and an out-of-plane torsional mode. The C=C stretching acts as both the promoting and accepting modes and it should dominate the radiationless decay in the EE and EZ isomers, due to their more planar configuration in S<sub>1</sub>. The torsional mode can act as an additional accepting mode in the decay of S<sub>1</sub> with a strongly out-of-plane distorted configuration, as in the case of the ZE and ZZ isomers.

The effect of temperature on *k*<sub>IC</sub>, observed for the isomers with the anthryl group in the cis position (from (2–3) × 10<sup>8</sup> to 4 × 10<sup>7</sup> s<sup>-1</sup> at 354 and 77 K, respectively), is probably due to higher nonadiabatic and diabatic terms of low-frequency vibrational modes (including the twisting of the rings around the single bond), thermally populated, effective in coupling S<sub>0</sub>–S<sub>1</sub>, as suggested for *n*-styrylpyridines<sup>18</sup> and their butadiene analogues.<sup>11</sup>

As stated above, the two lowest excited singlet states of “anthracene-like” nature are different in character, namely L<sub>b</sub> and (L<sub>a</sub>–B<sub>u</sub>) for S<sub>1</sub> and S<sub>2</sub>, respectively, as shown by the *k*<sub>F</sub> values of 9AnPhBs. The presence of the butadiene chain causes a preferential stabilization of the <sup>1</sup>L<sub>b</sub>\* state, as observed in polyenes,<sup>1a</sup> diphenylpolyenes,<sup>1a</sup> dithienylpolyenes,<sup>12,30</sup> and 2-anthrylphenylbutadienes.<sup>10</sup> Therefore, it gives rise to an inversion of the energy ordering of the two lowest excited states in 9AnPhBs, with respect to ethene analogues, whose S<sub>1</sub> state has a (L<sub>a</sub>–B<sub>u</sub>) nature.<sup>2,8</sup> The forbidden radiative transition becomes partially allowed by vibronic coupling of S<sub>1</sub> and S<sub>2</sub>.<sup>9,29,31</sup>

For all the isomers of 9AnPhB, the *k*<sub>ISC</sub> value is about 10<sup>7</sup> s<sup>-1</sup>, and it results to be lower than in the ethene analogues. The enhancing effect of the anthryl group on ISC decreases in the butadiene derivatives, showing that the degree to which larger polycyclic rings affect the excited-state properties decreases with increasing the chain length.<sup>9,12</sup>

## Conclusions

The spectral, photophysical, and photochemical behavior of the four geometrical isomers of 9AnPhB allowed us to obtain a fairly clear scheme of the competition of the relaxation processes of their lowest excited states of singlet and triplet multiplicity. The comparison between these results and those previously obtained for the ethene analogues<sup>2,8</sup> and diphenylbutadienes<sup>1a</sup> shows several similarities but also some important differences in the behavior of these compounds, due to the contemporaneous presence of the anthryl group and butadiene chain in the molecular skeleton.

The peculiar effect of the anthryl group, observed on the photobehavior of the ethene analogues<sup>2,8</sup> with respect to that of stilbenes,<sup>2,7</sup> is also preserved in these diene derivatives. The low S<sub>1</sub> and T<sub>1</sub> energies of the anthryl chromophore leads to a high torsional barrier for intramolecular rotation in the excited states, particularly for both *all-trans* geometries, <sup>1</sup>EE\* and <sup>3</sup>EE\*, which do not isomerize, even at high temperature. Furthermore, the other stereoisomers, with one or both double bonds in cis geometries, show a change in the isomerization pathway, from a prevalent diabatic singlet mechanism of DPhBs<sup>1a</sup> to a mixed (diabatic/adiabatic) triplet mechanism of these anthryl deriva-

tives. The insertion of a butadiene chain and an anthryl group in the molecular skeleton changes the shape of the potential energy curve as a function of the torsional coordinate. For these isomers, this curve should not experience a deep minimum at 90° after twisting (perpendicular geometry), but a very shallow minimum or even a saddle point, which can produce competition between the “horizontal” <sup>3</sup>perp\* → <sup>3</sup>trans\* and “vertical” <sup>3</sup>perp\* → <sup>1</sup>perp processes,<sup>32</sup> thus involving adiabatic and/or diabatic pathways in the deactivation of the T<sub>1</sub> state. Only the ZZ → ZE process proceeds through a diabatic singlet mechanism in the nonpolar solvent at room temperature.

The anthryl group also affects the S<sub>1</sub> → T<sub>1</sub> ISC process, increasing the *k*<sub>ISC</sub> rate parameter with respect to the corresponding phenyl analogues, even if this process becomes less important for longer chain compounds.

The presence of the butadiene chain causes a decrease of the radiative rate parameter in these dienes with respect to ethene analogues, owing to the change in the character of the lowest excited singlet state [from <sup>1</sup>(L<sub>a</sub>–B<sub>u</sub>)\* in 9StAns to <sup>1</sup>L<sub>b</sub>\* in 9AnPhBs].

The internal conversion is the main deactivation channel of the S<sub>1</sub> state, particularly for the isomers with one or two double bonds in the cis position, because in the latter compounds, with a strongly out-of-plane configuration, the torsional mode (twisting of the rings around the single bond), which can act as an additional accepting mode in the decay of S<sub>1</sub>, is also involved.

**Acknowledgment.** This research was funded by the Ministero per l'Università e la Ricerca Scientifica e Tecnologica (Rome) and the Perugia University in the framework of the Programmi di Ricerca di Interesse Nazionale (project: Mechanisms of Photoinduced Processes in Organized Systems). We are grateful to Prof. Ugo Mazzucato for stimulating discussions, Prof. Guido Galiazzo (Padua University), who prepared the samples, and Mr. Danilo Pannacci for his technical assistance.

## References

- (1) (a) Allen, M. T.; Whitten, D. G. *Chem. Rev.* **1989**, *89*, 1691 and references therein. (b) Saltiel, J.; Sun, Y.-P. In *Photochromism: Molecules and Systems*; Dürr, H., Bouas-Laurent, H., Eds.; Elsevier: Amsterdam, 1990; p 64.
- (2) Bartocci, G.; Mazzucato, U.; Spalletti, A.; Orlandi, G.; Poggi, G. *J. Chem. Soc., Faraday Trans.* **1992**, *88*, 3139 and references therein.
- (3) For review articles, see: (a) Zechmeister, L. *Experientia* **1954**, *10*, 1. (b) Hudson, B. S.; Köhler, B. E. *Annu. Rev. Phys. Chem.* **1974**, *25*, 437. (c) Hudson, B. S.; Köhler, B. E.; Shulten, K. In *Excited States*; Lim, E. C., Ed.; Academic Press: New York, 1982; Vol. 6, p 1. (d) Kawski, A.; Gryczynski, Z.; Gryczynski, I.; Wiezk, W.; Malok, H. Z. *Naturforsch.* **1991**, *45A*, 621. (e) Kawski, A.; Kubicki, A.; Kuklinski, B.; Gryczynski, I.; Gryczynski, Z. Z. *Naturforsch.* **1992**, *47A*, 1017. (f) Kawski, A.; Kuklinski, B.; Kubicki, A.; Gryczynski, I. Z. *Naturforsch.* **1992**, *47A*, 1204. (g) Orlandi, G.; Zerbetto, F.; Zgierski, M. Z. *Chem. Rev.* **1991**, *91*, 867.
- (4) Bensasson, R. V.; Land, E. J.; Truscott, T. G. *Excited States and Free Radicals in Biology and Medicine*; Oxford University Press: Oxford, 1993; p 201.
- (5) Mazzucato, U. *Pure Appl. Chem.* **1982**, *54*, 1705.
- (6) Mazzucato, U.; Aloisi, G. G.; Elisei, F. *Proc. Ind. Acad. Sci.* **1993**, *105*, 475.
- (7) Mazzucato, U.; Spalletti, A.; Bartocci, G.; Galiazzo, G. *Coord. Chem. Rev.* **1993**, *125*, 251.
- (8) Bartocci, G.; Spalletti, A.; Mazzucato, U. *Res. Chem. Intermed.* **1995**, *21*, 735.
- (9) Bartocci, G.; Galiazzo, G.; Gennari, G.; Marri, E.; Mazzucato, U.; Spalletti, A. *Chem. Phys.* **2001**, *272*, 213.
- (10) Spalletti, A.; Bartocci, G.; Galiazzo, G.; Macchioni, A.; Mazzucato, U. *J. Phys. Chem. A* **1999**, *103*, 8994.
- (11) Bartocci, G.; Galiazzo, G.; Mazzucato, U.; Spalletti, A. *Phys. Chem. Chem. Phys.* **2001**, *3*, 379.
- (12) Bartocci, G.; Spalletti, A.; Becker, R. S.; Elisei, F.; Floridi, S.; Mazzucato, U. *J. Am. Chem. Soc.* **1999**, *121*, 1065.

- (13) Meech, S. R.; Phillips, D. *J. Photochem.* **1983**, *23*, 193.
- (14) Bartocci, G.; Masetti, F.; Mazzucato, U.; Spalletti, A.; Baraldi, I.; Momicchioli, F. *J. Phys. Chem.* **1987**, *91*, 4733.
- (15) Galiazzo, G.; Spalletti, A.; Elisei, F.; Gennari, G. *Gazz. Chim. Ital.* **1989**, *119*, 277.
- (16) (a) Becker, H.-D.; Sandros, K.; Hansen, L. *J. Org. Chem.* **1981**, *46*, 821. (b) Becker, H.-D.; Hansen, L.; Andersson, K. *J. Org. Chem.* **1981**, *46*, 5419. (c) Becker, H.-D.; Andersson, K. *J. Org. Chem.* **1983**, *48*, 4543; **1985**, *50*, 3913.
- (17) Ogawa, K.; Suzuki, H.; Futakami, M. *J. Chem. Soc., Perkin Trans. 2* **1988**, 39.
- (18) Marconi, G.; Bartocci, G.; Mazzucato, U.; Spalletti, A.; Abbate, F.; Angeloni, L.; Castellucci, E. *Chem. Phys.* **1995**, *196*, 383.
- (19) Birks, J. B. *Photophysics of Aromatic Molecules*; Wiley-Interscience: London, 1970; p 88, eq 4.22.
- (20) Bhattacharyya, K.; Chattopadhyay, S. K.; Baral-Tosh, S.; Das, P. K. *J. Phys. Chem.* **1986**, *90*, 2646.
- (21) Anger, I.; Sundahl, M.; Wennerström, O.; Sandros, K.; Arai, T.; Tokumaru, K. *J. Phys. Chem.* **1992**, *96*, 7027.
- (22) (a) Arai, T.; Karatsu, T.; Misawa, H.; Kuriyama, Y.; Okamoto, H.; Hiresaki, T.; Furuuchi, H.; Zeng, H.; Sakuragi, H.; Tokumaru, K. *Pure Appl. Chem.* **1988**, *60*, 989 and references therein. (b) Sandros, K.; Becker, H.-D. *J. Photochem. Photobiol.* **1987**, *39*, 301. (c) Görner, H. *J. Photochem. Photobiol. A: Chem.* **1988**, *43*, 263.
- (23) Spalletti, A.; Bartocci, G.; Elisei, F.; Mancini, V.; Mazzucato, U. *J. Chem. Soc., Faraday Trans.* **1997**, *93*, 211.
- (24) Yee, W. A.; Hug, S. J.; Kliger, D. S. *J. Am. Chem. Soc.* **1988**, *110*, 2164.
- (25) Murov, S. L.; Carmichael, I.; Hug, G. L. *Handbook of Photochemistry*; Dekker: New York, 1993; pp 70, 109.
- (26) Birks, J. B. *Photophysics of Aromatic Molecules*; Wiley-Interscience: London, 1970; p 103, eq 4.55.
- (27) (a) Hudson, B. S.; Köhler, B. E. *J. Chem. Phys.* **1973**, *59*, 4984. (b) Andrews, J. R.; Hudson, B. S. *J. Chem. Phys.* **1976**, *65*, 55.
- (28) Birks, J. B.; Tzipathi, G. N. R.; Lumb, M. D. *Chem. Phys.* **1978**, *33*, 185.
- (29) Hug, G.; Becker, R. S. *J. Chem. Phys.* **1976**, *65*, 55.
- (30) Birnbaum, D.; Köler, B. E.; Spangler, C. W. *J. Chem. Phys.* **1991**, *94*, 1684.
- (31) Spalletti, A.; Bartocci, G. *Phys. Chem. Chem. Phys.* **1999**, *1*, 5623.
- (32) Orlandi, G.; Negri, F.; Mazzucato, U.; Bartocci, G. *J. Photochem. Photobiol. A: Chem.* **1990**, *55*, 37.